IEEE Access
Multidisciplinary | Rapid Review | Open Access Journal

Received June 3, 2020, accepted June 25, 2020, date of publication July 2, 2020, date of current version July 14, 2020.

Digital Object Identifier 10.1109/ACCESS.2020.3006617

On Sea Ice/Water Discrimination by Airborne Weather Radar

ALEXEY NEKRASOV[1,2,3], ALENA KHACHATURIAN[1], EVGENY ABRAMOV[1,2], PAVOL KURDEL[4], MÁRIA GAMCOVÁ[3], JÁN GAMEC[3], AND MIKHAIL BOGACHEV[1]

[1]Department of Radio Engineering Systems, Saint Petersburg Electrotechnical University, 197376 Saint Petersburg, Russia
[2]Institute of Computer Technologies and Information Security, Southern Federal University, 347922 Taganrog, Russia
[3]Faculty of Electrical Engineering and Informatics, Technical University of Košice, 042 00 Košice, Slovakia
[4]Faculty of Aeronautics, Technical University of Košice, 041 21 Košice, Slovakia

Corresponding author: Alexey Nekrasov (alexei-nekrassov@mail.ru)

This work was supported by the Russian Science Foundation under Project 16-19-00172.

ABSTRACT We consider a conceptual approach for the applicability of airborne weather radar for the sea ice/water discrimination and estimation of the sea ice age. The sea ice/water discrimination method suited for the airborne weather radar utilization is based on finding the minimum statistical distance of the measured normalized radar cross sections within a wide azimuth sector to the geophysical model functions of the sea ice and water, respectively. The sea ice age classification is based on the comparison of the normalized radar cross section value at a given incidence angle to the lower normalized radar cross section boundaries for the first-, second-, and multi-year ice. Implementation of the proposed methodology is considered for the C-band airborne weather radar operated in the ground mapping mode as a scatterometer scanning in a wide azimuth sector up to $\pm 100°$. We show explicitly that the proposed approach provides the enhancement of the conventional airborne weather radar functionality for the sea ice/water discrimination and sea ice age estimation either using stand-alone or joint measurements.

INDEX TERMS Airborne weather radar, algorithms, normalized radar cross section, radar remote sensing, sea ice, sea surface.

I. INTRODUCTION

Recent advancement of the satellite remote sensing technology throughout the last decades led to the development and dissemination of global scale monitoring tools covering the entire Earth surface including distant regions, otherwise hardly reachable with the conventional tools, due to their remoteness and often extreme climate conditions. Ongoing climate changes accompanying global warming appear especially pronounced in the remote polar regions that in turn leads to an increased interest in the online monitoring of the sea ice coverage dynamics. In this connection, joint use of the satellite-based remote sensing instrumentation provides global coverage to detect the development of ice cracks, as well as detachments of floating ice, that is essential to ensure safe shipping in waters with partial ice coverage. In this turn, the data obtained with the spaceborne instruments could be supplemented by additional data provided with the airborne remote sensing instruments, this way leading to a more detailed picture of the sea ice coverage dynamics.

To obtain detailed information on the sea ice and water surface, as well as to perform the sea ice/water discrimination in polar regions, using a combination of visible, infrared, and microwave sensors is desirable. At the same time, due to the regional specifics and sensors' functionality, microwave instruments are still the primary sensors suitable for the operation in remote areas, due to their robustness to frequent cloud coverage and fog, full operability during prolonged polar nights, in marked contrast to optical instruments, as well as their ability to distinguish between sea ice and water surface, due to significant differences in their microwave backscatter properties.

These microwave sensors are of two types: passive and active. A microwave radiometer is a passive sensor, while Synthetic Aperture Radar (SAR) and Scatterometer are active sensors.

Microwave radiometers are used for estimation of the sea ice extent and concentration, as well as for the detection of areas covered by multi-year (MY) ice. Passive microwave

The associate editor coordinating the review of this manuscript and approving it for publication was Pia Addabbo.

sensors flown in polar orbits provide observations within a relatively wide swath and almost daily complete coverage of the polar regions while being characterized by relatively low spatial resolution (around 25 km).

Scatterometers and SARs are used for observation of the water surface and sea ice to perform sea wind retrieval and sea ice measurements and classification. Spaceborne scatterometer measurements are capable of covering larger areas in comparison with the SARs while providing much lower spatial resolution (typically 25–50 km). In contrast, SARs provide with a higher spatial resolution (100–500 m), while being also capable of small-scale processes such as leads, deformation, and polynyas detection. As SAR signatures are complicated, it is difficult to perform an automated retrieval of the sea ice concentration and extent. Thus, microwave scatterometers can be considered as primary sensors for polar remote sensing potentially complemented by other measuring instruments.

Operating over water, wind scatterometers provide information about the sea surface wind vector. The wind parameters retrieval is based on the absolute measurement of the normalized radar cross section (NRCS) of the water surface from different azimuth angles (either at different or at the same incidence angles depending on the scatterometer configuration and its mounting on either satellite or aircraft). A geophysical model function (GMF) represents the expected NRCS model for the particular frequency band and corresponding wave polarization, respectively. In fact, the water GMF represents the dependence of NRCS on the wind speed U, incidence angle θ, and azimuth angle α relative to the up-wind direction [1]. Usually, it can be presented analytically, although sometimes it is provided in the tabular form only. For example, CMOD7 [2], one of the recent C-band GMFs used in our study has only tabular representation.

In addition to the wind measurements, scatterometers are also used for the sea ice detection and characterization while operating over the ice-covered waters [3]. The ice GMF representing the dependence of the ice NRCS from the incidence angle and frequency band is used in that case. Discrimination of the sea ice types is also based on different properties of the sea ice backscatter. In particular, MY ice is typically characterized by higher NRCS values than the first-year (FY) ice at the same incidence angles [3].

Recently, the suitability of the airborne weather radars (AWR) for the wind vector estimation over the water surface while operating in the ground mapping mode as a scatterometer scanning in a wide azimuth sector during rectilinear flight, or as a scatterometer with a fixed antenna during circular flight has been demonstrated in [4]–[9]. As nowadays AWR belongs to the minimum equipment list even for most light aircraft, it appears generally attractive to use this already available instrument also for the retrieval of the wind vector over the sea surface as well as for the sea ice/water discrimination and sea ice characterization.

In this connection, in the following we consider the possibility of innovative functionality enhancement of the AWR to perform the sea ice/water discrimination and evaluation of the sea ice age (and/or thickness) while operating in the ground mapping mode as a scatterometer scanning in a wide azimuth sector, in addition to its typical navigation applications, following the measurement geometry and algorithm proposed below.

II. METHOD

A. AWR KEY FEATURES

AWRs are typically nose-mounted and operated in either X- or C-band [10]. Earlier AWRs operated with a vertical transmit and receive polarization (VV) in the weather mode and used a horizontal polarization in the ground mapping mode [11]. Modern AWRs and integrated radars also operated in these and other modes may use several polarizations to provide improved characteristics. Despite of the AWR dual polarization measurement possibility, in the following, we consider only its VV polarization application, as the C-band water GMF CMOD7 has been developed only for the VV polarization, and the used ice age classification method is based on the C-band sea ice GMF currently available only for the VV polarization.

In the ground mapping mode, the antenna has a large cosecant-squared elevation beam that is relatively wide (10°–30°) in the vertical plane and narrow (2°–6°) in the horizontal plane, and sweeping in the azimuth sector (up to ±100°) (Fig. 1). As the antenna is both roll and pitch stabilized, the plane of the beam scanning is constantly horizontal. Those features allow the AWR operated in the ground mapping mode as a scatterometer to measure the NRCS of the observed surface. Next, measured NRCSs can be used for the retrieval of the wind speed and direction over the sea with the wind algorithm [4]–[9], and, as we show below, for the sea ice/water discrimination and even for the sea ice age evaluation.

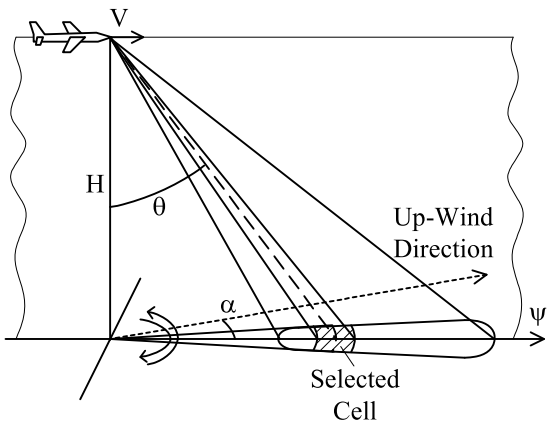

FIGURE 1. AWR scanning beam geometry.

B. SEA ICE/WATER DISCRIMINATION

Discrimination of the sea ice from water and estimation of both sea ice age and extent are based on differences between their NRSCs [12]. To perform the sea ice/water discrimination, there are several previously developed approaches, based on the anisotropy factor analysis [13], on the backscatter derivative estimate [14], on the minimum statistical distance between the measured NRCS values and the ice or water GMFs [15], as well as Bayesian-based approaches [16], [17] that are utilized either separately or in combination. Most of these methods have been implemented for the spaceborne scatterometers only.

To implement the sea ice/water discrimination, we propose to use the method which is based on finding the minimum statistical distance between the measured NRCS values in a wide azimuth sector and either the sea ice or the water GMFs when the summation results for the sea ice S_{ice} and water S_{water} are obtained by the least square method

$$\begin{cases} S_{ice} < S_{water} \Rightarrow \text{ice}, \\ S_{ice} > S_{water} \Rightarrow \text{water}, \\ S_{ice} \approx S_{water} \Rightarrow \text{uncertainty}, \end{cases} \tag{1}$$

where

$$S_{ice} = \sum_{i=1}^{N} \left(\sigma_i^{\circ *} - \sigma_{ice.i}^{\circ}\right)^2, \tag{2}$$

$$S_{water} = \sum_{i=1}^{N} \left(\sigma_i^{\circ *} - \sigma_{water.i}^{\circ}\right)^2, \tag{3}$$

$i = \overrightarrow{1, N}$, N is the number of scatterometer looks in different azimuthal directions at the same cell, $\sigma_i^{\circ *}$ is the i-measured NRCS, and $\sigma_{ice.i}^{\circ}$ and $\sigma_{water.i}^{\circ}$ are the closest values of the sea ice and water GMFs to the i-measured NRCS, respectively. The implementation of this approach requires the appropriate sea ice and water GMFs available for the given frequency band, as well as both transmit and receive electromagnetic wave polarization, respectively.

Recently, we have considered the sea ice/water discrimination method (1) with regard to its adaptation to the typical three fixed fan-beam geometry of a spaceborne scatterometer ASCAT [18]. For that purpose, the water GMF has been represented by CMOD7, and the sea ice GMF has been represented in the azimuthally isotropic form of [17], [20]

$$\sigma_{ice}^{\circ}(\theta) = \frac{1}{u(\theta)} \left(\sigma_{ice}^{\circ}(\theta_{ref}) + \int_{\theta_{ref}}^{\theta} u(\theta') A(\theta') d(\theta') \right), \tag{4}$$

where

$$u(\theta') = \exp\left(- \int_{\theta_{ref}}^{\theta'} B(\theta'') d(\theta'') \right), \tag{5}$$

$A(\theta)$ and $B(\theta)$ are the coefficients depending on the incidence angle and derived appropriately either for the Northern or for the Southern Hemispheres, respectively, θ_{ref} is the given reference incidence angle equal to 52.8° [17].

Due to the three fixed fan-beam ASCAT geometry, only three NRCSs $\sigma_1^{\circ *}$, $\sigma_2^{\circ *}$, and $\sigma_3^{\circ *}$ (fore-, mid-, and aft-beams, respectively) from three significantly different azimuth directions of 45°, 90°, and 135° relative to the satellite ground track are available for the same observation cell. Besides that, the mid-beam and the pair of fore- and aft-beams are oriented with different incidence angles. Accordingly, to implement the sea ice/water discrimination method (1) in the case of typical three fixed fan-beam geometry, the current water GMF parameters (the wind speed U and the up-wind direction α) that best fit to the measured NRCSs, the system of three equations has to be solved

$$\begin{cases} \sigma_1^{\circ *} = GMF(U, \theta_{\sigma_1^{\circ *}}, \alpha + \psi_{\sigma_1^{\circ *}}), \\ \sigma_2^{\circ *} = GMF(U, \theta_{\sigma_2^{\circ *}}, \alpha + \psi_{\sigma_2^{\circ *}}), \\ \sigma_3^{\circ *} = GMF(U, \theta_{\sigma_3^{\circ *}}, \alpha + \psi_{\sigma_3^{\circ *}}), \end{cases} \tag{6}$$

where $\theta_{\sigma_1^{\circ *}}$, $\theta_{\sigma_2^{\circ *}}$, and $\theta_{\sigma_3^{\circ *}}$ are the incidence angles corresponded to NRCSs obtained by the fore-, mid- and aft-beams from the same selected cell, $\psi_{\sigma_1^{\circ *}}$, $\psi_{\sigma_2^{\circ *}}$, and $\psi_{\sigma_3^{\circ *}}$ are the azimuthal angles of the cell selected by the appropriate beam relative to the satellite ground track.

Measurement geometries of the spaceborne scatterometers are absolutely different from the AWR observation geometry in the ground mapping mode. Spaceborne scatterometers are unable to provide with the azimuthal NRSC curves at the same incidence angles for the same selected cell (with the typical size of about 25–50 km) in the area observed, mainly due to their specific measurement geometry. As already noted above, typical fan-beam spaceborne scatterometers are limited to three fixed beams only. Therefore, they are capable of the selected cell observation from three azimuthal directions only, although at different incidence angles. As a result, they are unable to provide even with a sector of the NRCS curve for the same incidence angle in the ±90° azimuthal sector. A typical three-beam spaceborne scatterometer geometry also has a well-known disadvantage, as the wind vector retrieval can be ambiguous (providing from two to four wind directions) [19] especially when only a single polarization is used under measurements.

In marked contrast, the AWRs are free of the above limitations. In contrast to the spaceborne scatterometer geometries, the AWR wide-sector scanning geometry allows observation of the area of interest from significantly different azimuthal directions (up to ±100° relative to the aircraft course ψ), providing the NRCS measurements from many azimuthal directions at the same incidence angle, leading to an unambiguous retrieval of the wind vector [7]–[9].

Let an aircraft equipped with the AWR make a horizontal rectilinear flight with the speed V at some altitude H above the mean sea ice/water surface. Assuming the water/wind and ice conditions are more or less identical within the observed area which linear size does not exceed 15–20 km, the area can be considered to be identical to the selected cell by a

spaceborne scatterometer, while being observed from many significantly different directions in the sector of up to ±100°, e.g., with the azimuthal step of 10°. Then the number of scatterometer looks (integrated NRCSs) in different azimuthal directions will be equal to 19 (thus providing a much higher number of azimuthal looks than the satellite-based scatterometer).

Accordingly, for the sea ice/water discrimination method (1) in case of AWR scanning in the wide sector, the current water GMF parameters best fit to the measured NRCSs has to be found by solving the following system of $N = 19$ equations for the measured NRSCs

$$\begin{cases} \sigma_1^{\circ *} = GMF(U, \theta_{\sigma_1^{\circ *}}, \alpha + \psi_{\sigma_1^{\circ *}}), \\ \sigma_2^{\circ *} = GMF(U, \theta_{\sigma_2^{\circ *}}, \alpha + \psi_{\sigma_2^{\circ *}}), \\ \ldots\ldots\ldots\ldots\ldots\ldots\ldots\ldots\ldots \\ \sigma_{N-1}^{\circ *} = GMF(U, \theta_{\sigma_{N-1}^{\circ *}}, \alpha + \psi_{\sigma_{N-1}^{\circ *}}), \\ \sigma_N^{\circ *} = GMF(U, \theta_{\sigma_N^{\circ *}}, \alpha + \psi_{\sigma_N^{\circ *}}), \end{cases} \quad (7)$$

where $\theta_{\sigma_i^{\circ *}}$ is the incidence angle for the i-measured NRCS (assuming that all incidence angles are the same for AWR), $i = \overrightarrow{1, N}$, N is the number of scatterometer looks by AWR in different azimuthal directions, $\psi_{\sigma_i^{\circ *}}$ is the azimuthal angle between the aircraft course and the azimuthal direction of the i-measured NRCS.

Therefore, the sea ice/water discrimination method (1) looks more advantageous for application with AWR in comparison with its implementation on a three-beam spaceborne scatterometer in terms of both accuracy and spatial resolution, as we further confirm below using numerical simulations.

C. SEA ICE AGE EVALUATION

To evaluate the sea ice age (thickness) at various incidence angles with the help of (5), the sea ice NRCSs at a reference incidence angle can be used as a boundary condition for the scatterometer measurements. This kind of approach has been studied previously in [17] and applied for the sea ice age estimation from the European spaceborne scatterometers operated in a C-band with the VV polarization.

The NRCS lower boundaries as functions of the incidence angle for the FY, second-year (SY), and MY ice are presented in Fig. 2. They are exemplified for the Northern Hemisphere here, with the lower boundaries of the corresponding ice types at −21 dB, −16 dB, and −12 dB [21], respectively, at the reference incidence angle of 52.8°.

In the following, we focus on the numerical simulation that confirms the applicability of the above approach to the evaluation of the sea ice age with AWR.

III. RESULT

To evaluate the feasibility of the above approach for the AWR operated in the ground mapping mode as a scatterometer scanning in a wide azimuth sector, we next performed simulations considering CMOD7. Unfortunately, our simulations cover the VV polarization only, due to the availability of the corresponding GMF. We used the water GMF exemplified for

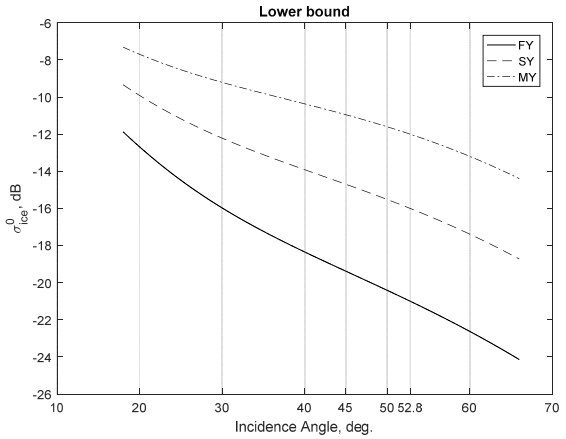

FIGURE 2. C-band VV polarization lower boundary curves for the Northern Hemisphere FY, SY, and MY sea ice types corresponding to the reference incidence angle of 52.8°: −21 dB, −16 dB, and −12 dB, respectively.

the 45° incidence angle shown in Fig. 3, as well as the sea ice GMF (4) with the coefficients for the Northern Hemisphere.

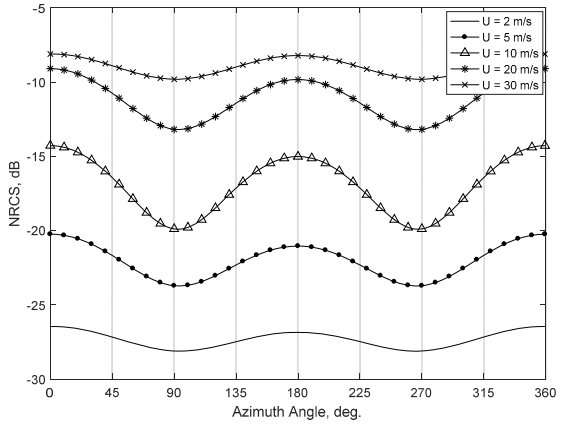

FIGURE 3. CMOD7 (C-band VV polarization) azimuthal curves for wind speeds of 2, 5, 10, 20, and 30 m/s at the incidence angle of 45°.

To demonstrate the feasibility of the sea ice/water discrimination with the AWR measurement geometry, we have simulated two particular scenarios, corresponding to the ice coverage and the water coverage, respectively. In case of the ice covered surface, the "measured" NRSCs have been generated using a Rayleigh Power (Exponential) distribution and integrated over 330 samples for each azimuthal direction in the sector of up to ±100° relative to the aircraft course with the azimuthal step of 10°. Next, to find the water GMF approximation, the wind speed and the up-wind direction, best fits to the "measured" NRSCs have been found by solving the system of $N = 19$ equations for "measured" NRSCs (7). Further, best fits of the ice GMF to the "measured" NRSCs are found and the sea ice/water discrimination is performed according to (1). Representative examples of the water and ice GMFs approximations in case of the ice surface are shown in Fig. 4.

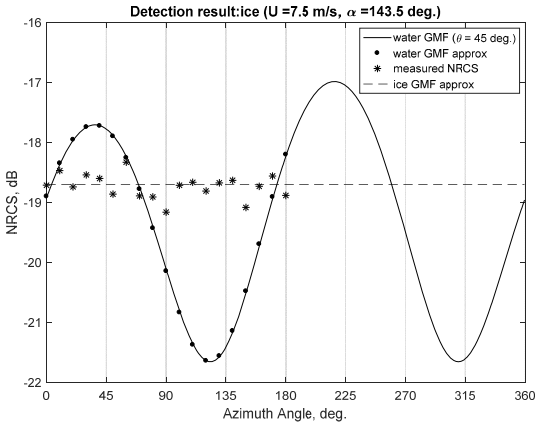

FIGURE 4. A simulation example of the water and ice GMFs approximations: ice surface case.

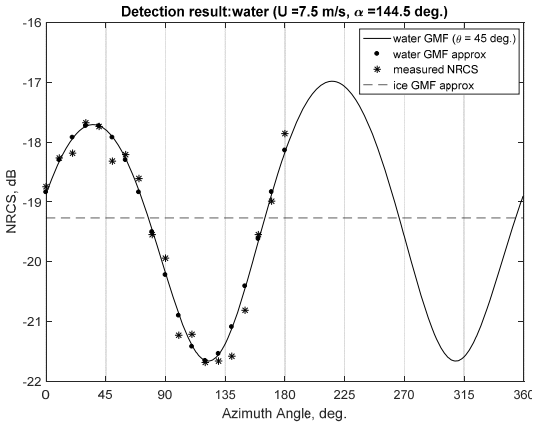

FIGURE 5. A simulation example of the water and ice GMFs approximations: water surface case.

Figure 4 clearly indicates that the sea ice GMF approximation fits much better with the ''measured'' NRCSs than the water GMF approximation. The calculated summation results for the sea ice and water are $7.14258 \cdot 10^{-6}$ and $2.54879 \cdot 10^{-4}$, respectively, that means that $S_{ice} < S_{water}$ and so in accordance with (1) the surface observed is classified as ice. Also, Fig. 4 demonstrates clearly that application of the sea ice/water discrimination procedure allows avoiding an uncertainty when the ''measured'' ice NRCS results will be perceived like wind over water (with the wind speed of 7.5 m/s and up-wind direction of 143.5° in our example).

The simulation result presented in Fig. 4 is for the Northern Hemisphere, and so we can see in Fig. 2 that in our simulation scenario the ''measured'' ice at the incidence angle of 45° is classified as the FY ice after the previous decision that the observed surface has been classified as the ice surface.

Since in the ice surface case the water GMF fitted the best to the ''measured'' ice NRSCs at the wind speed of 7.5 m/s and up-wind direction of 143.5°, we have used those wind parameters to choose the water GMF for the water surface case and then generate the ''measured'' NRSCs and integrate 330 NRCS samples for each azimuthal direction in the sector of up to ±100° relative to the aircraft course with the azimuthal step of 10°. Like in the previous case, to find the water GMF approximation, the wind speed and the up-wind direction providing best fits to the ''measured'' NRSCs have been found from the system of $N = 19$ equations (7). Then, best fits of the ice GMF to the ''measured'' NRSCs are found, and the sea ice/water discrimination is performed according to (1). Examples of the water and ice GMFs approximations corresponding to the water surface case are shown in Fig. 5.

Figure 5 clearly demonstrates that in the water surface case the water GMF approximation fits much better to the ''measured'' NRCSs than the sea ice GMF approximation. The calculated summation results for the sea ice and water are $2.47324 \cdot 10^{-4}$ and $7.10999 \cdot 10^{-6}$, respectively, that means that $S_{ice} > S_{water}$, and thus in accordance with (1) the observed surface is recognized as water. The wind parameters estimated from (7) indicated that the ''measured'' wind speed and the up-wind direction are 7.5 m/s and 144.5°, respectively. The ''measured'' wind speed is the same as the modeled wind speed, and ''measured'' up-wind direction differs from the modeled up-wind direction by 1° only.

Thus, the above two examples clearly indicate the ability and the efficacy of the sea ice/water discrimination by the algorithm developed for the AWR operating in the ground mapping mode as a scatterometer scanning in a wide azimuth sector or another airborne radar with similar features and geometry.

Assuming that wind and wave conditions in different parts of the observed area are identical, the measurement swath width, as well as the length of the area observed, should not exceed 15–20 km. This requirement leads to an altitude limitation for the method's applicability by AWR when expected that it may operate not only over sea ice but also over water. The maximum altitude limitation, in this case, will be about 10 km at the incidence angle of 45°, and 5 km at the incidence angle of 60°, respectively.

Further improvement of the sea ice/water discrimination and sea ice discrimination by the enhanced AWR can be achieved when appropriate C-band GMFs of the sea ice and water for the horizontal transmit and receive (HH) polarization will be developed to take the advantage of the dual VV and HH polarization measurement.

IV. CONCLUSION

To summarize, we have shown explicitly that either AWRs or other similar multi-mode radars operated in the ground mapping mode as a scatterometer scanning in a wide azimuth sector of up to ±100° can be used for the sea ice/water discrimination and evaluation of the sea ice age (thickness) in addition to its conventional application.

The method applied for the sea ice/water discrimination by the AWR is based on finding the minimum statistical distance between the measured NRCS values obtained within a wide azimuth sector and the sea ice/water GMFs that in turn is determined by the least mean square algorithm.

The sea ice and water GMFs for the appropriate frequency band and polarization are required for such applications. Lack of the reliable ice GMF and criteria for the sea ice age (thickness) classification does not allow for the evaluation of the sea ice age with the AWR, but its wide sector scanning geometry still could provide the sea ice/water discrimination just by obtaining the best average ice GMF approximation (represented by a horizontal line) that best fits to the measured NRCSs (according to the least squares criteria), and when the summation results for the sea ice will be lower than the summation results for the water.

Thus, the enhanced AWR or other multi-mode radars operated in the ground mapping mode as scatterometers scanning in a wide azimuth sector can be used either for the standalone, or for the joint spaceborne and airborne sea wind and ice measurement. We believe that the proposed solution could provide with an essential instrumental support both for the detailed sea ice coverage monitoring, as well as for the early detection of floating ice detachments important for safe shipping and other economic activities in the water areas with partial ice coverage.

ACKNOWLEDGMENT

The authors would like to express their sincere thanks to the Technical University of Košice for the research opportunities provided. Alexey Nekrasov would also like to thank the National Scholarship Program of the Slovak Republic for the support of an exchange visit.

REFERENCES

[1] E. G. Njoku, *Encyclopedia of Remote Sensing*. New York, NY, USA: Springer-Verlag, 2014, p. 939.
[2] *CMOD7*. Accessed: Jun. 26, 2020. [Online]. Available: http://projects.knmi.nl/scatterometer/cmod7
[3] F. T. Ulaby and D. G. Long, *Microwave Radar and Radiometric Remote Sensing*, Ann Arbor, MI, USA: University of Michigan Press, 2014, p. 1116.
[4] A. Nekrasov, "Water-surface wind vector estimation by an airborne weather radar having a medium-size scanning sector," in *Proc. 14th Int. Radar Symp. IRS*, Dresden, Germany, vol. 2, Jun. 2013, pp. 1079–1084. Accessed: Jun. 26, 2020. [Online]. Available: https://ieeexplore.ieee.org/document/6581724
[5] A. Nekrasov, *Foundations for Innovative Application of Airborne Radars: Measuring the Water Surface Backscattering Signature and Wind*. Dordrecht, The Netherlands: Springer, 2014, p. 116, doi: 10.1007/978-3-319-00621-5.
[6] A. Nekrasov and D. Popov, "A concept for measuring the water-surface backscattering signature by airborne weather radar," in *Proc. 16th Int. Radar Symp. (IRS)*, Dresden, Germany, Jun. 2015, pp. 1112–1116, doi: 10.1109/IRS.2015.7226252.
[7] A. Nekrasov, A. Khachaturian, V. Veremyev, and M. Bogachev, "Sea surface wind measurement by airborne weather radar scanning in a wide-size sector," *Atmosphere*, vol. 7, no. 5, 72, pp. 1–11, May 2016, doi: 10.3390/atmos7050072.
[8] A. Nekrasov and D. Popov, "A concept for measuring the water-surface backscattering signature by airborne weather radar," in *Proc. 16th Int. Radar Symp. (IRS)*, Dresden, Germany, vol. 2, Jun. 2015, pp. 1112–1116, doi: 10.1109/IRS.2015.7226252.
[9] A. Nekrasov and F. Dell'Acqua, "Airborne weather radar: A theoretical approach for water-surface backscattering and wind measurements," *IEEE Geosci. Remote Sens. Mag.*, vol. 4, no. 4, pp. 38–50, Dec. 2016, doi: 10.1109/MGRS.2016.2613840.
[10] M. Kayton and W. R. Fried, *Avionics Navigation Systems*, New York, USA: Wiley, 1997, p. 773.
[11] A. A. Sosnovsky, I. A. Khaymovich, E. A. Lutin, and I. B. Maximov, *Aviation Radio Navigation: Handbook*. Moscow, Russia: Transport (in Russian), 1990, p. 264.
[12] M. B. Rivas, I. Otosaka, A. Stoffelen, and A. Verhoef, "A scatterometer record of sea ice extents and backscatter: 1992–2016," *Cryosphere*, vol. 12, no. 9, pp. 2941–2953, Sep. 2018, doi: 10.5194/tc-12-2941-2018.
[13] A. Cavenié, F. Gohin, Y. Quilfen, and P. Lecomte, "Identification of sea ice zones using AMI wind: Physical bases and applications to the FDP and CERSAT processing chains," *Proc. 2nd ERS-1 Symp.*, Hamburg, Germany, vol. 361, Oct. 1993, pp. 1009–1012. Accessed: Jun. 26, 2020. [Online]. Available: https://earth.esa.int/documents/10174/1589798/ESA04+vol2.pdf
[14] F. Gohin, "Some active and passive microwave signatures of Antarctic sea ice from mid-winter to spring 1991," *Int. J. Remote Sens.*, vol. 16, no. 11, pp. 2031–2054, Jul. 1995, doi: 10.1080/01431169508954537.
[15] M. B. Rivas, J. Verspeek, A. Verhoef, and A. Stoffelen, "Bayesian sea ice detection with the Advanced Scatterometer ASCAT," *IEEE Trans. Geosci. Remote Sens.*, vol. 50, no. 7, pp. 2649–2657, Jul. 2012, doi: 10.1109/TGRS.2011.2182356.
[16] H. S. Anderson and D. J. Long, "Sea ice mapping method for SeaWinds," *IEEE Trans. Geosci. Remote Sens.*, vol. 43, no. 3, pp. 647–657, Mar. 2005, doi: 10.1109/TGRS.2004.842017.
[17] I. Otosaka, M. B. Rivas, and A. Stoffelen, "Bayesian sea ice detection with the ERS scatterometer and sea ice backscatter model at C-band," *IEEE Trans. Geosci. Remote Sens.*, vol. 56, no. 4, pp. 2248–2254, Apr. 2018, doi: 10.1109/TGRS.2017.2777670.
[18] A. Nekrasov, A. Khachaturian, E. Abramov, O. Markelov, and M. Bogachev, "On sea ice measurement by a C-band scatterometer at VV polarization: Methodology optimization based on computer simulations," *Remote Sens.*, vol. 11, no. 21, 2518, pp. 1–15, Oct. 2019, doi: 10.3390/rs11212518.
[19] I. Otosaka, M. B. Rivas, and A. Stoffelen, "Errata: Bayesian sea ice detection with the ERS scatterometer and sea ice backscatter model at C-band," *IEEE Trans. Geosci. Remote Sens.*, vol. 57, no. 12, p. 10447, Dec. 2019, doi: 10.1109/TGRS.2019.2928720.
[20] W. Lin, M. Portabella, A. Stoffelen, and A. Verhoef, "On the characteristics of ASCAT wind direction ambiguities," *Atmos. Meas. Tech.*, vol. 6, no. 4, pp. 1053–1060, Apr. 2013, doi: 10.5194/amt-6-1053-2013.
[21] M. B. Rivas, private communication, Jun. 2019.

ALEXEY NEKRASOV received the Diploma degree in radio engineering and the Ph.D. degree (Candidate of Technical Science) from the Taganrog State University of Radio Engineering (TSURE), Taganrog, Russia, in 1991 and 1998, respectively.

From 1991 to 1999, he was an Assistant Professor at the Taganrog State University of Radio Engineering (TSURE), Taganrog, where he held an academic title of Associate Professor, in 2000. Since 1999, he has been an Associate Professor at Southern Federal University (formerly TSURE), Russia. Since 2016, he has also been as a Senior Scientist at Saint Petersburg Electrotechnical University, Russia, and he is also with the Technical University of Košice, Slovakia. His research interests include sea and land remote sensing from aircraft and satellites, oceanography, sea winds, scattering from rough surfaces, radar system design, and information security.

Dr. Nekrasov has been an expert of the Russian Academy of Sciences, the Russian Science Foundation, the Fulbright Program in Russia, a recipient of 24 international grants and awards, and a reviewer for IEEE TRANSACTIONS ON GEOSCIENCE AND REMOTE SENSING, the IEEE GEOSCIENCE AND REMOTE SENSING LETTERS, the IEEE ANTENNAS AND WIRELESS PROPAGATION LETTERS, *Remote Sensing*, *Atmosphere*, *Climate*, *Symmetry*, *Journal of Marine Science and Engineering*, *IET Radar, Sonar & Navigation*, *IET Image Processing*, and *ISPRS International Archives of the Photogrammetry, Remote Sensing and Spatial Information Sciences*.

ALENA KHACHATURIAN received the Diploma degree in radio engineering and the Ph.D. degree (Candidate of Technical Science) from Saint Petersburg Electrotechnical University "LETI" (ETU), Saint Petersburg, Russia, in 2010 and 2014, respectively.

From 2010 to 2016, she was an Assistant Professor at the Radio Engineering Department, ETU, where she has been an Associate Professor and a Senior Researcher, since 2016. Her research interests include sea and land remote sensing, scattering from rough surfaces, radar systems, and global navigation satellite systems.

EVGENY ABRAMOV received the B.S. degree in computer networks, the M.S. degree in informatics, and the Ph.D. degree in information security from the Taganrog State University of Radio Engineering (TSURE), Taganrog, Russia, in 2000, 2001, and 2005, respectively.

In 2006, he was an Associate Professor at the Southern Federal University (SFedU) (formerly TSURE), Russia, where he has been the Head of the Department of Information Security, since 2013. He worked as a Research Fellow at the Institute of Engineering Physics, Serpukhov, Russia, and consecutively as a Senior Researcher and Leading Researcher in different projects of Southern Federal University. He is the coauthor of three book chapters and about 15 research articles in international journals. He also worked as a Visiting Professor at the University of Pisa, Italy, and the University of Informatics Sciences, Cuba. His research interests include cybersecurity, intrusion and anomaly detection, intrusion tolerant and active respond systems, artificial neural networks, machine learning, the IoT security, and remote sensing.

PAVOL KURDEL received the degree in electronics engineering from the Military Aviation Academy, Košice, Slovakia, in 2000, and the Ph.D. degree in electronics from the Technical University of Košice, in 2011.

From 2011 to 2014, he worked as an Assistant Professor at the Department of Avionics, Faculty of Aeronautics, Technical University of Košice, where he was the Vice-Dean of the Faculty of Aeronautics, from 2014 to 2017. In 2016, he was an Associate Professor in electronics with the Technical University of Košice, where he has been working as an Associate Professor, since 2017. He was a member of international projects within the EU, where the most important was the construction of a research and development facility for aircraft antenna research. His scientific interests include electronic aircraft systems, traffic ergonomic systems management, airport processes, and remote sensing. He is the author of 110 publications, including monographs, textbooks, patents, and articles indexed in WoS – Current Contents Connect, and Scopus.

Dr. Kurdel was a member of the Supervisory Board of Košice International Airport, from 2015 to 2017. He was a recipient of the medals and awards from the Minister of Defense of the Slovak Republic and the Faculty of Aeronautics.

MÁRIA GAMCOVÁ was born in Košice, Slovakia, in 1965. She received the M.S. degree in electrical engineering and the Ph.D. degree in radioelectronics from the Technical University of Košice, Slovakia, in 1989 and 2005, respectively.

From 1989 to 2019, she was an Assistant Professor at the Department of Electronics and Multimedia Communications, Technical University of Košice, where she has been an Associate Professor, since 2019. She holds one patent. Her research interests include theory of linear circuits, digital image processing, UWB radar signal processing, and remote sensing.

JÁN GAMEC was born in Stul'any, Slovakia, in 1960. He received the degree *(summa cum laude)* in radioelectronics and the Ph.D. degree in radioelectronics from the Technical University of Košice, Slovakia, in 1985 and 1995, respectively.

He is currently an Associate Professor at the Department of Electronics and Multimedia Communications, Faculty of Electrical Engineering and Informatics, Technical University of Košice. He holds one patent. His main areas of scientific research interests include digital image processing, UWB radar signal processing, low-profile antennas for UWB radars, and remote sensing.

MIKHAIL BOGACHEV received the B.S. and M.S. degrees in radio engineering systems, the Ph.D. degree in biomedical engineering, and the D.Sc. degree in mathematical modeling, numerical methods, and software development from St. Petersburg Electrotechnical University "LETI," St. Petersburg, Russia, in 2000, 2002, 2005, and 2018, respectively.

From 2006 to 2009, he was a Research Fellow at the Institute of Theoretical Physics, University of Giessen, Germany. From 2010 to 2019, he has been consecutively a Senior Researcher, an Associate Professor, and the Leading Researcher at the Radio Systems Department, St. Petersburg Electrotechnical University "LETI," where he is currently the Principal Researcher of the Centre for Digital Telecommunication Technologies and a Full Professor at the Radio Systems Department. He is the coauthor of five book chapters and more than 50 research articles in international journals. His research interests include data analytics and applied statistics with particular focus on time series analysis and complex systems dynamics with broad interdisciplinary applications to bioinformatics and computational biology, climate, geosciences and remote sensing, telecommunication networks, as well as physiology and medicine.

Dr. Bogachev was a recipient of several grant awards by the Ministry of Science and Higher Education of the Russian Federation, by the Russian Science Foundation, and by the Russian Foundation for Basic Research, as a Principal Investigator, as well as a Co-Supervisor of a bilateral German-Russian Research Project. He is also a frequent reviewer of several multidisciplinary and physics journals, including *Nature Communications*, *Science of the Total Environment*, *Scientific Reports*, *PLoS One*, *Applied Mathematical Modelling*, *New Journal of Physics*, *Physical Review*, *EPL*, and *Physica*.